Journal of Ovonic Research Vol. 18, No. 1, January - February 2022, p. 11- 20

First principles study the effect of Zn doped MgO on the energy band gap using GGA approximation

A. M. Ghaleb[a*], R. A.Munef [a], S. F. Mohammed[b]
[a]*Department of physics, college of science, University of Kirkuk, Iraq*
[b]*Department of Electricity, Technical Institute of Kirkuk, Iraq*

The structural, electronic, and optical properties were investigated by performing first-principles calculations within the framework of density functional theory (DFT) for zinc-saturated magnesium oxide ($Zn_xMg_{1-x}O$) with different concentrations of Zn (x = 0, 0.125, 0.375 and 0.5). The crystal structure used in this calculation was the cubic MgO with a space group of Fm-3m with a 2x1x1 supercell. An increase in the zinc concentration increased the lattice parameters of $Zn_xMg_{1-x}O$ and reduced the band gap of the material. The absorption function and refractive index were improved with increasing doping concentration of Zn in the $Zn_xMg_{1-x}O$ compared to pure MgO. In addition, this information could provide a direction in the fabrication of a good photo catalyst material.

(Received October 16, 2021; Accepted January 8, 2022)

Keywords: Density functional theory, Electronic properties, Optical properties, Zn doping, MgO

1. Introduction

The mineral MgO is the second most abundant in the lower Earth mantle and under normal conditions, MgO crystallizes in the rock salt structure [1]. MgO is an important ceramic oxide is a transparent insulator widely used investigated in many fields that have undergone many experimental and theoretical studies[2]. MgO is characterized by a high melting point, low expansion coefficients and low thermal conductivity, and there is also a growing trend to use MgO as a substrate for thin-film growth and as an optical material. MgOis highly ionic with a minor structure of NaCl [3]. Major research interest in renewable and clean energy has emerged over the past few decades [4-6]. The fuel cell is one of the most interesting sources of energy. Hydrogen plays a major role in the electrochemical reaction of the fuel cell [7-10]. Several theoretical and experimental approaches have been performed on Zn-doped MgO, where doping of Zn into MgO leads to a reduction in the band gap and an improvement in the optical properties at lower excitation energies. The band gap of Zn-doped MgO can be tuned in the range from 3.3 to 7.8 eV [11]. From a theoretical point of view, Wang et al. Al [12] simulated Zn-doped MgO using the GW method based on multiparticle perturbation theory to correct the DFT band structure. Hu et. [13]. In this work, we simulate Zn-doped ($Zn_xMg_{1-x}O$) at four different concentrations (x = 0, 0.125, 0.375 and 0.500), using the MgO super cell method. The position of zinc is determined by calculating the minimum energy for each potential site using density functional theory (DFT). For the band structure calculations for Zn - doped, calculations of optical properties such as refractive index and absorption are included in this work to explore the behavior of these materials in photo catalytic activity, the aim of this study is to reduce the energy band gap by doping it with zinc.

* Corresponding author: abdlhadik@uokirkuk.edu.iq
https://doi.org/10.15251/JOR.2022.181.11

2. Method of calculation

DFT is used in theoretical studies that are carried out in Cambridge flat-wave voltage false total energy (CASTEP) [14]. The ultra-soft pseudo potential is used to describe the interaction between an electron-ion [15]. MgO belongs to the Fm-3m space group having a face-centered cubic (FCC) composition with lattice parameters a = 4.2121 Å.Fig.1. shows the theoretical model for the crystal structure of undoped MgO. The green ball represents Mg atoms, and the red ball represents O atoms. the calculations are performed using the ultra-soft pseudo potential technique with electronic valence configurations of $Mg(2p^6 3s^2)$ and $O(2s^2 2p^4)$.The GGA -PW91 approximation [16] was used for the exchange relationship between electrons and the cut off energy of a plane wave equal to 400 eV. Monk horst-Pack (MP) k-meshes of $3 \times 6 \times 6$ face-centered cubic structures are used to ensure total energy convergence within 5×10^{-6} eV/atom

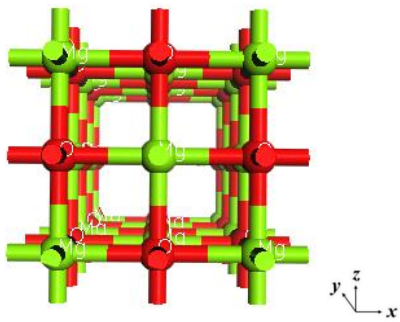

Fig. 1. $2 \times 1 \times 1$ MgO *supercell,where the green balls represent* Mg *atom, and red balls represent* O *atom.*

2. Result and Discussion

2.1. Electronic properties

After performing the optimization process for the structure of MgO, $Zn_{0.125}Mg_{0.875}O$, $Zn_{0.25}Mg_{0.75}O$, $Zn_{0.375}Mg_{0.625}O$, and $Zn_{0.5}Mg_{0.5}O$, and presented in Table 1, it is shown that any increase in the concentration of Zn increases the volume of the MgO compound. The increase in the lattice constant confirms the formation of Zn-doped MgO.

Table 1. Structural parameters of MgO, $Zn_{0.125}Mg_{0.875}O$, $Zn_{0.250}Mg_{0.750}O$, $Zn_{0.375}Mg_{0.625}O$, *and* $Zn_{0.500}Mg_{0.500}O$.

Zn Concentration	Lattice Parameter (A°)	Volume ($A^{\circ 3}$)	$\frac{V}{V_\circ}$	Mg − O (Å)	Zn − O (Å)	E_g (eV)
0	4.29486	79.22187	1.0607	2.14742		4.284
0.125	4.29897	79.4621	1.064		2.12889	2.731
0.250	4.30115	79.683	1.0696	2.1252	2.18202	2.324
0.375	4.30502	79.9193	1.0712	2.13429	2.18623	2.023
0.500	4.30850	80.1525	1.0732	2.13497	2.18278	1.599

According to Vegard's law which states that there is a linear relationship between the crystal lattice constant of the alloy and the concentrations of the component elements under the constant temperature condition which is considered an approximate empirical rule [17]. Zn-doped MgO was created by replacing one of the Mg atoms with one of the Zn atoms as shown in Fig.2.The unit cell in MgO consists of 4 atoms each of O and Mg, this means that there are 4 different positions of the Mg atom that can be replaced by Zn atom. The value of the lattice constant increases linearly with the increase in the concentration of Zn in MgO. The ionic radius of $Zn^{+2}$and Mg^{+2} are 0.74 Å,0.71Å[18] respectively. This means that the radius of Zn^{+2} isa bit larger than the radius of Mg^{+2} . The reason why the lattice constant of Zn-doped MgO shifts toward larger values with increasing Zn concentration is likely due to the replacement of Mg^{+2} ions by Zn^{+2} ions in the MgO lattice.

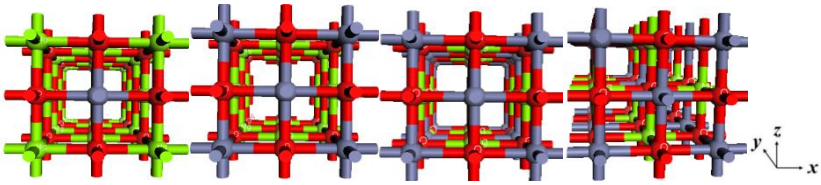

Fig. 2. Crystal structures of Zn- doped MgO with different concentration of Zn, where the green balls represent Mg atom, silver balls represent Zn atom and red balls represent O atom.

The calculated electronic band structures along the Γ- F- Q - Z - Γ direction in the high-symmetry Brillouin region of MgO were shown in Fig.3, respectively. The electronic band gap calculation shows that the direct MgO band gap has the highest value of 4.284 eV with Γ − Γ direction.

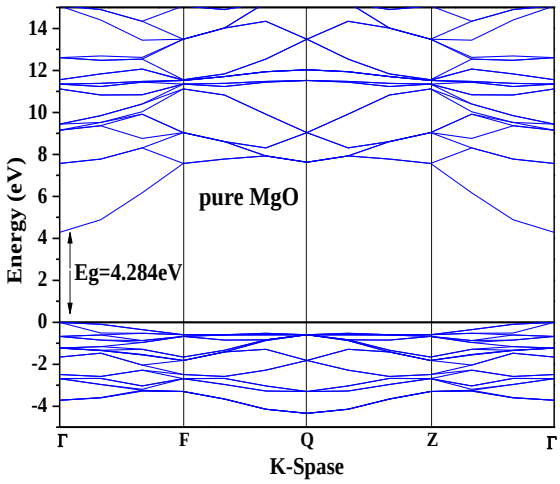

Fig. 3. Calculated band structure of pure MgO using GGA -PW91aproxmation.

For Zn-doped MgO, the electronic band structure around the Brillouin region along the symmetry lines was shown in Fig.4(a-d),where the doping value of Zn was set as 0.125, 0.25,0.375, and 0.5. It is found that the band gap values decrease with increasing Zn concentration in MgO about 2.685eV. The decreases in the band gap according to (GGA- Pw91) calculations is observed when the Zn concentration increases from 0.0 to 0.125, which becomes 1.553eV, from 0.125 to 0.25, 0.407eV, from 0.25 to

0.375,0.301eV,and from 0.375 to 0.5, 0.424eV. Thus, the introduction of Zn into MgO can narrow the band gap of the obtained solid semiconductor and expand the light absorption from ultraviolet to visible light, potentially improving the photo catalytic performance of Zn_xMg_{1-x} O.

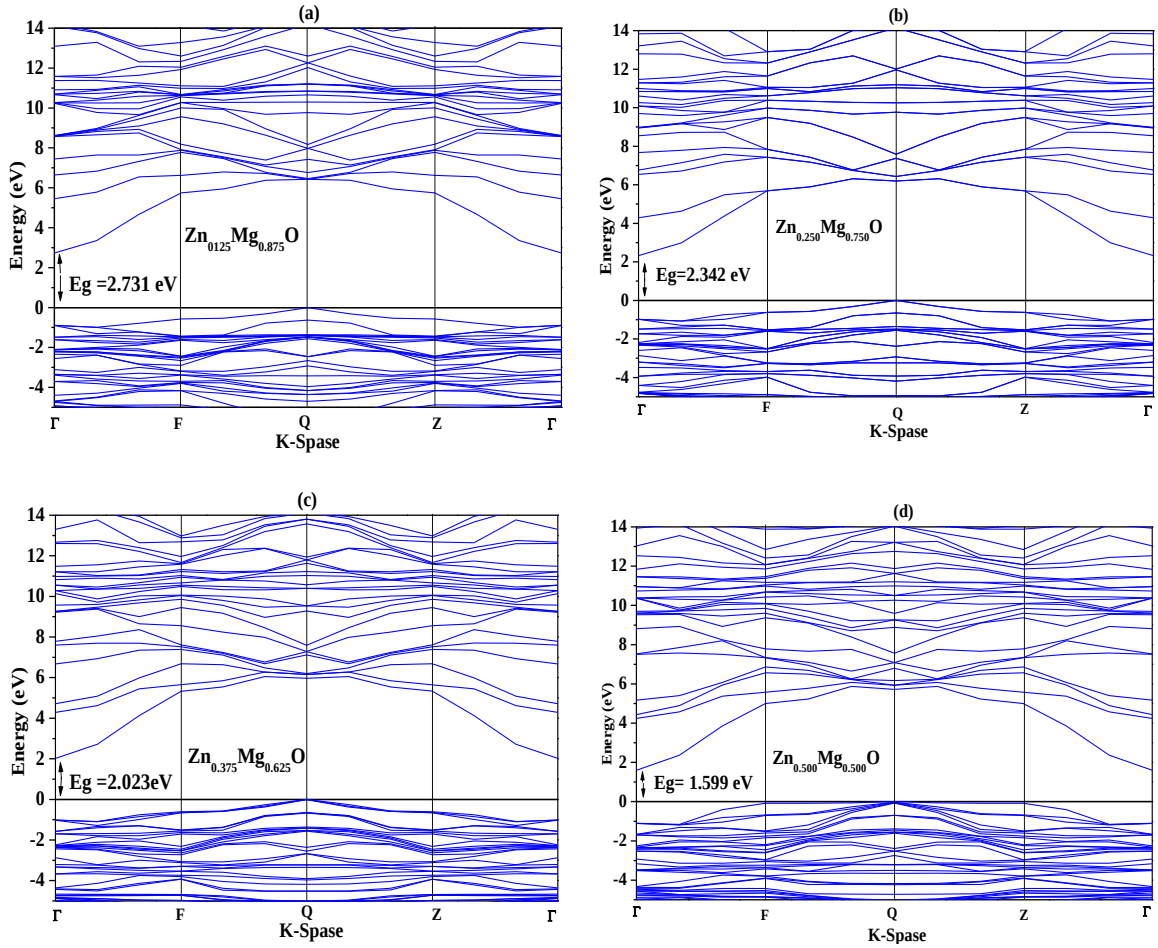

Fig. 4. Calculated band structure of $Zn_xMg_{1-x}O$ using GGA +PW91aproxmation.

Fig.5a shows the Partial Density of States (PDOS) of all atoms in pure MgO, from PDOS, the maximum valence band (VB_{Max}) near the Fermi level is mainly contributed to theO_{2P}state, while in the conduction band (CB) there is a small appearance of Mg_{2P} and Mg_{3S} states, which indicates the ionic nature of the bonds between Mg and O atoms. The conduction band consists of antibonding states O_{2P} in addition to the contribution of Mg atoms as well. The deep region of the valence band consists of the O_{2S} state far from the occupied bands with a gap of about 11 eV. For Zn-doped MgO Fig.5b, the fermi level moved towards the conduction band due to the high contribution of the impurity energy level (IEL) from the Zn_{3d} state. The impurity energy formation of Zn narrows the band gap. A low contribution from the Zn_{3d}state appears in the valence band (VB) while the high contribution from the Zn_{3d} state can be seen in the lower part of the conduction band. The IEL position made IEL become shallow donor level. This type of IEL can act as a trap center for holes or photo excited electrons which can reduce the recombination rate. The Zn_{3d} states in the conduction band overlap with theO_{2P}states, indicating a strong exchange interaction between them. The projected (PDOS) for atoms O and Mg are also shown. The

calculated band gap of 4.284 eV directly at Γ point , it is smaller than the experimentally reported gap of 7.8eV [19], and close to other recent calculations [20]. The total width of the upper VB is about 5.1eV, this is in good agreement with the experiment result. The lower Mg_{2P} and O_{2S} of the VB have a width of (1.6, 2.1) eV and peaks at (-39.1, -15.7) eV respectively. The CB also has two peaks, one at 9.8eV and the other much sharper at 11.7eV. There is a large degree of hybridization between the Mg and O.

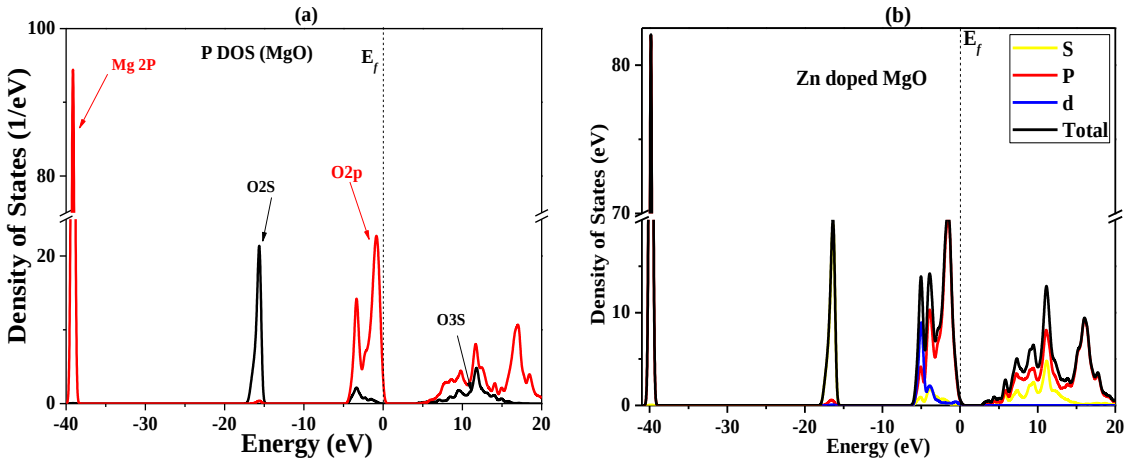

Fig. 5. Calculated (a) PDOS of MgO ,(b) PDOS of Zn-doped MgO.

2.2. Optical properties

To study the interactions that occur between incident photons and the compound $Zn_xMg_{1-x}O$ using the optical property, it is important physical parameters for use in research and instrumentation applications [21-25]. The dielectric function describes the optical response of a substance at different photon energy. The real part $\varepsilon_1(\omega)$ can be calculated by the Kramer-Krönig relationship, which connects $\varepsilon_1(\omega)$ and the imaginary part $\varepsilon_2(\omega)$.The function $\varepsilon_2(\omega)$ can be calculated from the elements of the matrix in the wave function for occupied and unoccupied states. Other optical parameters, such as Extinction coefficient ($\mathbf{K(\omega)}$), Reflectance ($\mathbf{R(\omega)}$), Refractive index ($\mathbf{n(\omega)}$), and Absorption coefficient, it is obtained from $\varepsilon_1(\omega)$ and $\varepsilon_2(\omega)$. The buffer function is given as:

$$\varepsilon(\omega) = \varepsilon_1(\omega) + i\varepsilon_2 \tag{1}$$

$$\varepsilon_1(\omega) = 1 + \frac{2}{\pi} p \int_0^{\infty} \frac{\omega' \varepsilon_2(\omega)}{\omega'^2 - \omega^2} d\omega' \tag{2}$$

$$\varepsilon_2(\omega) = -\frac{2\omega}{\pi} p \frac{\varepsilon_1(\omega')}{\omega'^2 - \omega^2} d\omega' \tag{3}$$

$$\alpha(\omega) = \sqrt{2}[\sqrt{\varepsilon_1{}^2(\omega) + \varepsilon_2{}^2(\omega)} - \varepsilon_1(\omega)]^{\frac{1}{2}} \tag{4}$$

$$R(\omega) = \frac{\left|\sqrt{\varepsilon(\omega)} - 1\right|^2}{\left|\sqrt{\varepsilon(\omega)} + 1\right|^2} \tag{5}$$

$$n(\omega) = \frac{1}{\sqrt{2}}\left[(\varepsilon_1^2(\omega) + \varepsilon_2^2(\omega))^{\frac{1}{2}} + \varepsilon_1(\omega)\right]^{\frac{1}{2}} \quad (6)$$

$$K(\omega) = \frac{1}{\sqrt{2}}\left[(\varepsilon_1^2(\omega) + \varepsilon_2^2(\omega))^{\frac{1}{2}} - \varepsilon_1(\omega)\right]^{\frac{1}{2}} \quad (7)$$

where p represents the Cauchy principal value of the integral [26], $\varepsilon_1(\omega)$ represents the energy storage capacity of the material and $\varepsilon_2(\omega)$ shows the absorption behavior and electronic band structure [27]. Fig.6(a,b) shows the imaginary and real part of the isolation function for $Zn_xMg_{1-x}O$within the photon energy range from 0-20 eV. From Fig.6a the observed different peaks of $\varepsilon_2(\omega)$are due to the direct transitions of electrons from the VB to the CB along the symmetric lines of Γ- F – Q – Z - Γ. The threshold energy of $\varepsilon_2(\omega)$ is 3.23, 2.81, 2.63, 2.36 and 2.21eV for MgO, $Zn_{0.125}Mg_{0.875}O, Zn_{0.250}Mg_{0.750}O, Zn_{0.375}Mg_{0.625}O$, and $Zn_{0.500}Mg_{0.500}O$, respectively, which is the basic absorption edge of solid solutions, corresponding to the transitions of electrons from VB_{Max} to CB_{Min} at high points of symmetry (ie the bandgap). Where $\varepsilon_2(\omega)$ increases with increasing energy and shows strong absorption peaks in the energy range 11–12.6 eV. Table. 2 shows the maximum values of $\varepsilon_2(\omega)$ in the high energy range, this means that $Zn_xMg_{1-x}O$ can be used as an energy filter in the Ultraviolet (UV) spectrum. Fig. 6b. shows the contrast of the real part $\varepsilon_1(\omega)$ of the dielectric function of $Zn_xMg_{1-x}O$ versus the photon energy.

2.3. Absorption coefficient (α (ω)):

The optical absorption coefficient plays an effective role in determining the photo catalytic activity, as the absorption coefficient determines the penetration of light of a particular wavelength before it is absorbed by the material. In Fig.6c, the absorption coefficient (ω) is shown for MgO and $Zn_xMg_{1-x}O$ at (x = 0.125, 0.25, 0.375, 0.5) for the energy of a photon. The optical absorption of MgO in the UV light region occurs by electron transfer from the O_{2P} orbital of valence band to the Mg_{3S} orbital of conduction band. The intensities of the prominent peaks of the $Zn_xMg_{1-x}O$ adsorption values at (x = 0, 0.125, 0.25,375,0.5) are (4.282, 2.731, 2.324, 2.023, 1.599) eV respectively. Thus, it indicates that the increase in the concentration of steroids led to a slightly increased absorption. The so-called red shift occurs where the absorption edges of Zn-doped MgO shift towards a lower energy region in visible light. A significant red shift of $Zn_xMg_{1-x}O$ towards visible light occurs at a low concentration of x = 0.125. The red shift of the absorption edge occurs because of the large changes in the electronic structures, which is due to the change in the composition of the energy bands and the introduction of impurity states. Therefore, the electrons in the VB can be excited to the CB by absorbing visible light. This will make the Zn-doped MgO ideal for efficient solar energy utilization in the visible light region which improves the photo catalytic activity.

2.4. Reflectance ($R(\omega)$):

Fig. 6d, shows the reflectivity of $Zn_xMg_{1-x}O$ against the photon energy. The calculated values of static reflectivity for $MgO, Zn_{0.125}Mg_{0.875}O, Zn_{0.25}Mg_{0.75}O$ $, Zn_{0.375}Mg_{0.625}O,$ and $Zn_{0.5}Mg_{0.5}O,$ are 0.930, 0.102, 0.11, 0.119 and 0.128, respectively. The reflectivity of $Zn_xMg_{1-x}O$ increases directly with the photon energy until it a reaches the maximum value in the energy range of 13.8–18.8eV, The R (ω) of

the material describes its surface roughness. The spectral behavior of R (ω) is delineated in Fig. 6d. The results show that when the value of $\varepsilon_1(\omega)$ contains negative values, R(ω) obtains a larger value. The highest value of R(ω) was obtained for $Zn_xMg_{1-x}O$, which indicates that this material is used as a favorable coating candidate for reducing solar heating [28].

2.5. Refractive index ($n(\omega)$):

The refractive index is one of the important physical properties of a material, as determining and knowing the refractive index of a semiconductor is very useful for designing devices [29-33].From Fig.6e, there is a similarity between the direction of refractive index $n(\omega)$ and the direction of $\varepsilon_1(\omega)$ with the energy of the photon. The constant values of $n(\omega)$ are 1.87, 1.94, 1.99, 2.05 and 2.12 for MgO, $Zn_{0.125}Mg_{0.875}O$, $Zn_{0.25}Mg_{0.75}O$, $Zn_{0.375}Mg_{0.625}O$, and $Zn_{0.5}Mg_{0.5}O$, respectively. The $n(\omega)$ values increase for $Zn_xMg_{1-x}O$ also with the photon energy at first similar to $\varepsilon_1(\omega)$, then decreasing with increasing energy and decreasing below unity with little oscillations, this means that the group velocity (V_g) where ($V_g = \frac{c}{n}$) of the incident ray is greater than (c: speed of light).The $n(\omega)$ of $Zn_xMg_{1-x}O$ at its various concentrations reach their maximum values in the energy range 4.87- 6.32eV, which corresponds to the maximum absorption of the substance as listed in Table .2.

2.6. Extinction coefficient ($K(\omega)$):

The extinction coefficient of a material is directly related to its absorption modulus. The extinction coefficient of the $Zn_xMg_{1-x}O$ was presented against the photon energy Fig.6f. The critical points are 3.92, 2.54, 2.19, 1.91, and 1.57 eV for the spectra of MgO, $Zn_{0.125}Mg_{0.875}O$, $Zn_{0.125}Mg_{0.875}O$, $Zn_{0.25}Mg_{0.75}O$, $Zn_{0.375}Mg_{0.625}O$, and $Zn_{0.5}Mg_{0.5}O$ respectively . The $K(\omega)$ values for $Zn_xMg_{1-x}O$ gradually increase with the photon energy above and reach peak values in the energy range of 11.2–13.8eV showing maximum absorption.

Table2.Calculated static $\varepsilon_1(0)$, $\varepsilon_1(\omega)_{Max}$, refractive index (n(0)), $n(\omega)_{Max}$,Reflectance ($R(\omega)$), and absorption edge of extinction coefficient K(ω)for $Zn_xMg_{1-x}O$

Optical properties	MgO	$Zn_{0.125}Mg_{0.875}O$	$Zn_{0.25}Mg_{0.75}O$	$Zn_{0.375}Mg_{0.625}O$	$Zn_{0.5}Mg_{0.5}O$
$\varepsilon_1(0)$	3.51	3.7	3.97	4.21	4.47
$\varepsilon_1(\omega)_{Max}$	6.22	5.61	5.42	5.25	4.79
$\varepsilon_2(\omega)_{Max}$	11eV	11.3eV	11.6eV	12.4eV	12.6eV
n(0)	1.87	1.94	1.99	2.05	2.12
$n(\omega)_{Max}$	1.87eV	1.94eV	1.99eV	2.05eV	2.12eV
R(0)	0.93	0.102	0.11	0.119	0.128
$k(\omega)_{Max}$	11.2eV	13.5eV	13.6eV	13.7eV	13.8eV

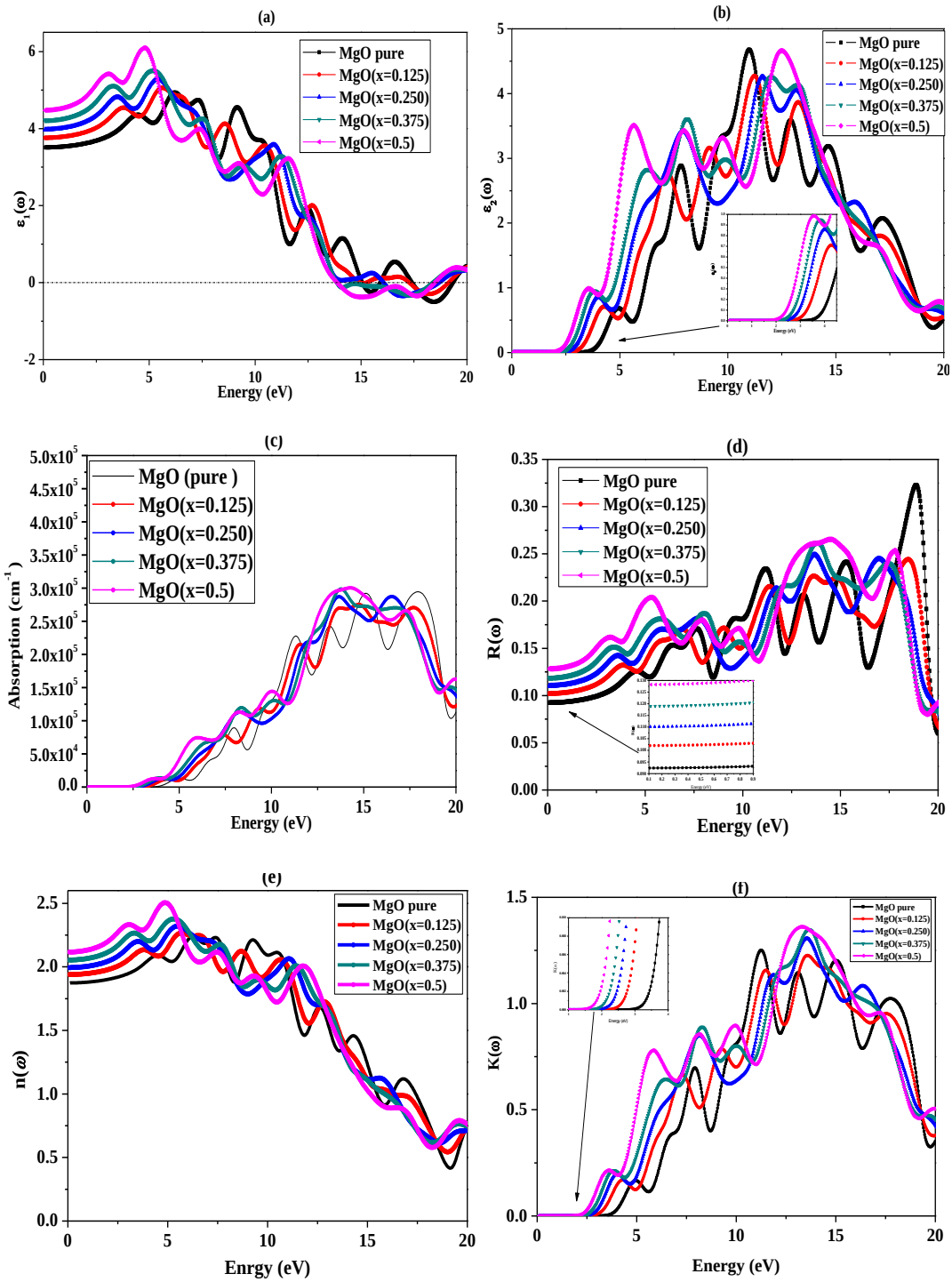

Fig. 6. Show static $\varepsilon_1(0)$, $\varepsilon_1(\omega)_{Max}$, refractive index (n(0)), $n(\omega)_{Max}$,Reflectance $(R(\omega))$, and absorption edge of extinction coefficient K(ω)for $Zn_xMg_{1-x}O$

3. Conclusion

Using a first principles study based on DFT the structural, electronic and optical properties of pure MgO and - doped MgO were calculated. Using the exchange correlation function (GGA-Pw91) in the simulation program CASTEP. The wide band gap of pure MgO made it have low optical absorption, thus to improve its optical properties, the Zn atom was replaced by Mg.

The (GGA-Pw91) function was used as the exchange correlation function to report the properties of Zn-doped MgO,because it shows the value of the lattice parameter and the band gap close to the experimental values. The absorption edges of Zn-doped MgO shifted with increasing the concentration of Zn towards the longer wavelengths spectrum extending from UV light, as the absorption coefficient of Zn-doped MgO decreased and the band gaps of MgO decreased. These results give a good explanation for the red shift of light absorption in Zn-doped MgO may also be of use in understanding the atomic level of the structural, electronic and optical properties of MgO and Zn-doped MgO. In summary the photo catalytic activity was significantly improved after MgO was doped with Zn.

References

[1]A.GboyegaA.debayo, Yunfeng Liang, Caetano R. Miranda, SandroScandolo, The Journal of chemical physics 131(1),014506 (2009); https://doi.org/10.1063/1.3146902

[2]Jong Wan Lee, Jae-HyeonKo, Journal of Information Display 15(4), 157 (2014); https://doi.org/10.1080/15980316.2014.955140

[3]Yong-NianXu, W. Y. Ching, Physical Review B 43(5),4461 (1991); https://doi.org/10.1103/PhysRevB.43.4461

[4] K. Tromly, Renewable Energy: An Overview, Energy Effic. Renew. Energy Clear, (2001).

[5] E. Walz, S. Energy, E. Walz, Nat. Biotechnol. (2009).

[6] V. Khare, S. Nema, P. Baredar, Sustain. Energy Rev. (2016).

[7] Y. Wang, K.S. Chen, J. Mishler, S.C. Cho, X.C. Adroher, Appl. Energy. (2011).

[8] Fuel Cell Technologies Office (FCTO), Fuel cell technologies office multiyear research, development and demonstration plan, U.S. Dep. Energy. (2016). doi:Department of Energy.

[9] J. Larminie, A. Dicks, Fuel Cell Systems Explained, 2001.

[10] S.M.J. Zaidi, M.A. Rauf, Polym. Membr. Fuel Cells, 2009.

[11] J. Wang, Y. Tu, L. Yang, H. Tolner, J. Comput. Electron. 15, 1521 (2016); https://doi.org/10.1007/s10825-016-0906-2

[12] H.C. Hsu, C.Y. Wu, H.M. Cheng, W.F. Hsieh, Appl. Phys. Lett. (2006).

[13] Y. Hu, B. Cai, Z. Hu, Y. Liu, S. Zhang, H. Zeng, Curr. Appl. Phys. (2015).

[14] K. Maeda, K. Teramura, D. Lu, T. Takata, N. Saito, Y. Inoue, K. Domen, Nature, (2006).

[15] L. Liao, Q. Zhang, Z. Su, Z. Zhao, Y. Wang, Y. Li, X. Lu, D. Wei, G. Feng, Q. Yu, X. Cai, J. Zhao, Z. Ren, H. Fang, F. Robles-Hernandez, S. Baldelli, J. Bao, Nat. Nanotechnol. (2014).

[16] J.P. Perdew, Phys. Rev. B 33, 8822 (1986); https://doi.org/10.1103/PhysRevB.33.8822

[17]Alan R.Denton, Neil W. Ashcroft, Physical review A 43(6), 3161 (1991); https://doi.org/10.1103/PhysRevA.43.3161

[18]Jan Spielmann, DirkPiesik, Bernd Wittkamp, Georg Jansen, Sjoerd Harder, Chemical communications23, 3455 (2009); https://doi.org/10.1039/b906319f

[19] D. M. Roessier, W. C. Walker, Physical Review 159(3), 733 (1967); https://doi.org/10.1103/PhysRev.159.733

[20]Mohamad Fariz, Mohamad Taib, SamatMohdHazrie, S. Z. N. Demon, HussinNur Hafiz, Hassan Oskar Hasdinor, YahyaMuhdZuAzhan, Ali Ab Malik Marwan, First-principles study on the doping effects of La on the structural, electronic and optical properties of MgO,(2020).

[21] S. Adachi, J. Appl. Phys 58,R1 (1985); https://doi.org/10.1063/1.336070

[22] N. Bouarissa, Mater. Sci.Eng. B 86,53 (2001); https://doi.org/10.1016/S0921-5107(01)00658-4

[23] S. Adachi, Properties of Group-IV, III-V, and II-VI Semiconductors, Wiley, Chichester,2005; https://doi.org/10.1002/0470090340

[24] S. Adachi, Properties of Semiconductor Alloys: group-IV, III-V and II-VISemiconductors, John Wiley & Sons Ltd., Chichester, 2009.

[25] A. Bouarissa, A. Gueddim, N. Bouarissa, S. Djellali, Polym. Bull 75,3023 (2018); https://doi.org/10.1007/s00289-017-2189-6

[26]LiYanlu, Xian Zhao, Weiliu Fan, The Journal of Physical Chemistry C 115(9), 3552 (2011); https://doi.org/10.1021/jp1098816

[27] S. Hussain, G. Murtaza, S.H. Khan, A. Khan, M.A. Ali, M. Faizan, A. Mahmood,R. Khenata, Mater. Res. Bull. 79,73(2016); https://doi.org/10.1016/j.materresbull.2016.03.001

[28] H. Shafique , S. A. Aldaghfag , M. Kashif , M. Zahid , M.Yaseen , J. Iqbal , Misbah , R. Neffati,Chalcogenide Letters ,18, 589 (2021).

[29] S. Ozaki, S. Adachi, J. Appl. Phys 75, 7470 (1994); https://doi.org/10.1063/1.356617

[30] K. I. Suzuki, S. Adachi, J. Appl. Phys83,1018 (1998); https://doi.org/10.1063/1.366791

[31] N. Bouarissa, Mater. Chem. Phys 72, 387 (2001); https://doi.org/10.1016/S0254-0584(01)00304-2

[32] N. M. Ravindra, P. Ganapathy, J. Choi, Infrared Phys. Technol50,21 (2007); https://doi.org/10.1016/j.infrared.2006.04.001

[33] N. Bouarissa, Mater. Chem. Phys 73,51 (2002); https://doi.org/10.1016/S0254-0584(01)00347-9